Available online at www.qu.edu.iq/journalcm
JOURNAL OF AL-QADISIYAH FOR COMPUTER SCIENCE AND MATHEMATICS
ISSN:2521-3504(online) ISSN:2074-0204(print)

Analysis of the MHD Oscillatory Flow and Its Effect on the Temperature and Concentration of Ree-Eyring Fluid Between Two Parallel Horizontal Porous Plates

Sadiq A. Mohammad AL-Husainy [a,*], Dheia G. Salih Al-Khafajy [b]

[a,b]Department of Mathematics, College of Science, University of Al-Qadisiyah, Diwaniya, Iraq.
[a] E-mail: sci.math.mas.23.1@qu.edu.iq
[b] E-mail: dheia.salih@qu.edu.iq

ARTICLE INFO

Article history:
Received: 4 /3/2025
Rrevised form: dd /mm/2025
Accepted : 10 /04 /2025
Available online: 30 /06/2025

Keywords:

Ree-Eyring fluid, Magnetohydrodynamic (MHD), parallel plate, perturbation technique.

ABSTRACT

This work aims to examine the effects of magnetohydrodynamic (MHD) oscillatory flow on heat transfer and concentration in a Ree-Eyring fluid within a channel bounded by two parallel porous plates. The problem is formulated as a nonlinear, nonhomogeneous partial differential equation. The momentum equation is solved using the separation of variables method combined with the perturbation technique to determine the velocity, temperature, and concentration profiles. The obtained solutions are analyzed using MATHEMATICA 14.1, with graphical representations illustrating the results. The analysis is conducted using various parameter values to explore their influence on the system.

MSC..

https://doi.org/10.29304/jqcsm.2025.17.22203

1. Introduction

The study and analysis of non-Newtonian fluid flow and their rheological properties are multidisciplinary topics with broad application areas. In fact, the behavior of non-Newtonian fluids is observed in nearly every chemical and related manufacturing industry. These fluids are utilized in thermal extrusion systems, biomedical engineering, and other fields. The factors determining the properties of non-Newtonian fluids are highly complex, and understanding them requires significant effort from researchers. The application areas are also vast and diverse, demanding substantial input. Applications in thermal technology, such as crude oil

*Corresponding author: Sadiq A. Mohammad AL-Husainy

Email addresses: *sci.math.mas.23.1@qu.edu.iq*

Communicated by 'sub editor'

refineries, heat exchangers, and insulation systems, rely on the efficient transfer of heat and mass within well-defined fluid systems. Many physicists, chemists, and engineers work in this field [6]. No single equation can fully describe the physical and mathematical properties of non-Newtonian fluids. The effect of the electric field generated by an electric current is an important topic in the study of fluid flow through various channels. This has prompted many researchers to explore the applications of these phenomena across multiple scientific fields that impact human life [2]. Several studies have examined the oscillatory flow of fluids through parallel plates exposed to a magnetic field. For instance, Soundalgekar and Bhat [3] investigated the oscillatory magnetohydrodynamic flow and heat transfer of a non-Newtonian fluid inside a channel. Attia and Kotb [4] analyzed the continuous motion of an electrically conductive, viscous, incompressible fluid between two parallel horizontal plates. Additionally, Khadir and Al-Khafaji [5] studied heat exchange in oscillatory flows of Williamson fluid through a porous surface under different flow configurations. Furthermore, some studies have focused on Ree-Eyring fluid, a class of non-Newtonian fluids, and investigated its flow under varying conditions, through different channels, and over distinct time periods, as illustrated in works such as [10-13]. Oscillatory magnetohydrodynamic (MHD) flow analysis is an advanced research area in fluid dynamics, focusing on the interaction between magnetic fields and fluid motion. In this study, we investigate the effects of oscillatory MHD flow on the temperature distribution and concentration of Ree-Eyring fluid between two horizontal parallel porous plates. Ree-Eyring fluid, characterized by its non-Newtonian viscosity properties, serves as an ideal model for analyzing complex hydrodynamic phenomena in porous environments. Partial differential equations are used to model the interactions among magnetic, thermal, and concentration forces, taking into account the effects of thermal conductivity, diffusion, and variable viscosity [6, 7]. The study of oscillatory flow in non-Newtonian fluids is of great importance in various engineering applications. Previous research has shown that magnetic fields can significantly influence velocity, temperature, and concentration distributions in fluids, particularly in porous media [8, 9]. In this work, we propose a mathematical model to analyze the effects of oscillatory MHD flow of Ree-Eyring fluid between two parallel plates on the fluid's temperature and concentration. By solving the governing equations for momentum, energy, and mass conservation, we examine the impact of various parameters on velocity, temperature, and concentration profiles. Dimensionless parameters, such as the Peclet number, are employed to characterize heat and mass transfer processes. Using MATHEMATICA 14.1, we plot velocity, temperature, and concentration profiles for both Poiseuille and Couette flow scenarios, providing a comprehensive visualization of the system's dynamics.

Mathematical Formulation

A magnetic field, influenced by the presence of a simple electric current, was applied to a fluid stream flowing between two parallel horizontal porous plates to develop a mathematical model governing the oscillatory flow of a Ree-Eyring fluid. The channel has a width h, with the upper wall subjected to a temperature T_1 and a fluid concentration C_1, while the lower wall has a temperature T_0 and a fluid concentration C_0 , as shown in Figure 1. The flow is considered in two cases: stationary (Poiseuille flow) and moving at a constant velocity (Couette flow). Cartesian coordinates were employed, where x_1 represents the horizontal axis and x_2 the vertical axis, defining the flow field as $(V_1(x_2,t),0,0)$ which satisfies the continuity equation.

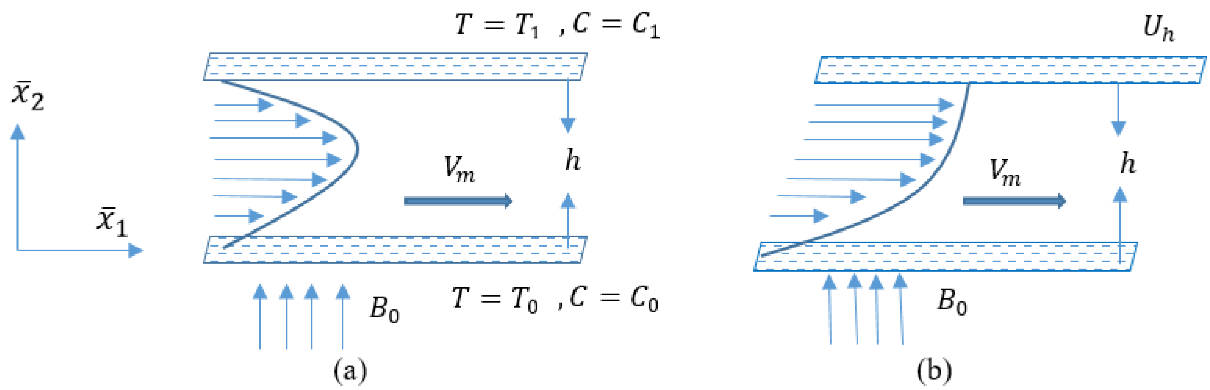

Figure (1) Channel format: (a) Poiseuille flow and (b) Couette flow

The basic equations for the problem [1]:

$$\frac{\partial \bar{V}_1}{\partial \bar{x}_1} + \frac{\partial \bar{V}_2}{\partial \bar{x}_2} = 0 \tag{1}$$

$$\rho\left(\frac{\partial \bar{V}_1}{\partial \bar{t}} + \bar{V}_1 \frac{\partial \bar{V}_1}{\partial \bar{x}_1} + \bar{V}_2 \frac{\partial \bar{V}_1}{\partial \bar{x}_2}\right) = -\frac{\partial \bar{p}}{\partial \bar{x}_1} + \frac{\partial \bar{\tau}_{12}}{\partial \bar{x}_2} - \sigma B_0^2 \bar{V}_1 - \frac{\mu_0}{k} \bar{V}_1 \tag{2}$$

$$\rho\left(\frac{\partial \bar{V}_2}{\partial \bar{t}} + \bar{V}_1 \frac{\partial \bar{V}_2}{\partial \bar{x}_1} + \bar{V}_2 \frac{\partial \bar{V}_2}{\partial \bar{x}_2}\right) = -\frac{\partial \bar{p}}{\partial \bar{x}_2} + \frac{\partial \bar{\tau}_{21}}{\partial \bar{x}_1} - \sigma B_0^2 \bar{V}_2 - \frac{\mu_0}{k} \bar{V}_2 \tag{3}$$

$$\rho \frac{\partial T}{\partial \bar{t}} = \frac{K}{C_p} \frac{\partial^2 T}{\partial \bar{x}_2{}^2} + \bar{\tau}_{12} \frac{\partial \bar{V}_1}{\partial \bar{x}_2} - \frac{1}{C_p} \frac{\partial q}{\partial \bar{x}_2} \tag{4}$$

$$\frac{\partial C}{\partial \bar{t}} = D \frac{\partial^2 C}{\partial \bar{x}_2{}^2} - K_r^*(C - C_0) + \frac{D K_H}{T_m} \frac{\partial^2 T}{\partial \bar{x}_2{}^2} \tag{5}$$

The above equations represent, respectively, the continuity equation, the momentum equation, the temperature equation, and the concentration equation, Where $(\bar{V}_1)$ is the axial velocity, (T) is a fluid temperature, (B_0) is a magnetic field strength, (μ_0) is a zero shear rate viscosity, (ρ) is a fluid density, (σ) is a conductivity of the fluid, (k) is a permeability, (c_p) is a specific heat at constant pressure, (K) is a thermal conductivity and (q) is a radioactive heat flux, (C) is the concentration, (K_H) is the thermal diffusion ratio, (D) is the coefficient of mass diffusivity, (T_m) the mean fluid temperature.

The temperatures and concentration at the walls of the channel are given as:

$$T = T_0 \text{ at } \bar{x}_2 = 0\,, \text{ and } T = T_1 \text{at } \bar{x}_2 = h \tag{6}$$

$$C = C_0 \text{ at } \bar{x}_2 = 0\,, \text{ and } C = C_1 \text{ at } \bar{x}_2 = h \tag{7}$$

The radioactive heat flux given by [9]:

$$\frac{\partial q}{\partial \bar{x}_2} = 4\eta^2 (T_0 - T) \tag{8}$$

The radiation absorption denoted by η.

The fundamental equation for the Ree-Eyring fluid given by [2]:

$$\tau_{ij} = \left[\mu_0 \frac{\partial V_i}{\partial x_j} + \frac{1}{\acute{B}} sinh^{-1}\left(\frac{1}{\acute{C}} \frac{\partial V_i}{\partial x_j}\right)\right]$$

Since $sinh^{-1}(\text{Å}) \cong \text{Å} - \frac{\text{Å}^3}{3!}$ for $|\text{Å}| \ll 1$, we have $\tau_{ij} = \left[\mu_0 \frac{\partial V_i}{\partial x_j} + \frac{1}{\acute{B}}\left(\frac{1}{\acute{C}} \frac{\partial V_i}{\partial x_j} - \frac{1}{3!}\left(\frac{1}{\acute{C}} \frac{\partial V_i}{\partial x_j}\right)^3\right)\right]$ and for the velocity vector $(V_1(x_2, \text{t}), 0\,, 0)$, we get

$$\tau_{ij} = \begin{cases} \left[\mu_0 + \frac{1}{\acute{B}\acute{C}}\right] \frac{\partial V_1}{\partial x_2} - \frac{1}{3!\acute{B}\acute{C}^3}\left(\frac{\partial V_1}{\partial x_2}\right)^3 & i = 1 \text{ and } j = 2 \\ 0 & otherwise \end{cases} \tag{9}$$

Method of solution

To simplify the governing equations of the problem, we introduce the following dimensionless transformations:

$$\left.\begin{array}{c} x_1=\frac{\bar{x}_1}{h},\ x_2=\frac{\bar{x}_2}{h}, V_1=\frac{\bar{V}_1}{V_m}, V_2=\frac{\bar{V}_2}{V_m}, \theta=\frac{T-T_0}{T_1-T_0}, t=\frac{\bar{t}\,V_m}{h}, Re=\frac{\rho h\,V_m}{\mu_0} \\ \Phi=\frac{C-C_0}{C_1-C_0}, e_1=\frac{1}{\mu_0\acute{B}\acute{C}}, e_2=\frac{e_1}{3!}\left(\frac{V_m}{\acute{C}h}\right)^2, U_0=\frac{U_h}{V_m},\ \tau_{12}=\frac{h}{\mu_0\,V_m}\bar{\tau}_{12}, p=\frac{\bar{p}h}{\mu_0\,V_m} \\ Pe=\frac{\rho h\,V_m c_p}{K}, N^2=\frac{4\eta^2h^2}{K}, Da=\frac{k}{h^2}, M^2=\frac{\sigma B_0^2h^2}{\mu_0}\ , Gr=\frac{\rho g\beta h^2(T_1-T_0)}{\mu_0\,V_m} \end{array}\right\} \tag{10}$$

Where (V_m) is the mean flow velocity, (Da) is the Darcy number, (Re) is the Reynolds number, (Gr) is the Grashof number, (M) is the magnetic parameter, (Pe) is the Peclet number, and (N) is the radiation parameter, while (e_1) and (e_2) are the Ree-Eyring fluid parameters.

By substituting equation (10) in equations (8) and (9), and then substituting from there into equations (1 – 5), we have

$$\frac{\partial V_1}{\partial x_1}+\frac{\partial V_2}{\partial x_2}=0 \tag{11}$$

$$Re\frac{\partial V_1}{\partial t}=-\frac{\partial p}{\partial x_1}+[1+e_1]\frac{\partial^2 V_1}{\partial {x_2}^2}-3e_2\left(\frac{\partial V_1}{\partial x_2}\right)^2\frac{\partial^2 V_1}{\partial {x_2}^2}-\left(M^2+\frac{1}{Da}\right)V_1 \tag{12}$$

$$\frac{\partial p}{\partial x_2}=0 \tag{13}$$

$$Pe\frac{\partial \theta}{\partial t}=\frac{\partial^2\theta}{\partial {x_2}^2}+Br\left([1+e_1]\left(\frac{\partial V_1}{\partial x_2}\right)^2-e_2\left(\frac{\partial V_1}{\partial x_2}\right)^4\right)+N^2\theta \tag{14}$$

$$\frac{\partial \Phi}{\partial t}=\frac{1}{S_c}\frac{\partial^2\Phi}{\partial {x_2}^2}-K_r\Phi+S_r\frac{\partial^2\theta}{\partial {x_2}^2} \tag{15}$$

Solution of the Problem

A. To solve the motion equation (12), for two types of flow (Poiseuille flow and Couette flow). From equation (13), the pressure function does not depend on x_2, and then let

$$V_1(x_2,t)=v_1(x_2)e^{i\omega t}\text{ and }-\frac{dp}{dx_1}=\lambda e^{i\omega t} \tag{16}$$

Where λ is a real constant and ω is the oscillation frequency. Substituting equation (16) into equation (12), after simplifying the result, we obtain;

$$[1+e_1]\frac{\partial^2 v_1(x_2)}{\partial {x_2}^2}-3e_2e^{2i\omega t}\left(\frac{\partial v_1(x_2)}{\partial x_2}\right)^2\frac{\partial^2 v_1(x_2)}{\partial {x_2}^2}-\left(M^2+\frac{1}{Da}+R_e i\omega\right)v_1(x_2)=-\lambda \tag{17}$$

Which is a nonhomogeneous nonlinear differential equation, and it is difficult to find an exact solution, so we will use the perturbation technique to find the solution of the equation (17) by taking a small value for e_2. Accordingly, we write

$$v_1=v_{10}+e_2\,v_{11}+O({e_2}^2) \tag{18}$$

Substituting equation (18) into equation (17), then by equating the similar powers of e_2, we get the following results:

$$\frac{\partial^2 v_{10}}{\partial {x_2}^2}-\left(\frac{M^2+\frac{1}{Da}+R_e i\omega}{[1+e_1]}\right)v_{10}=-\left(\frac{\lambda}{[1+e_1]}\right)\qquad\text{(zero - order)} \tag{19}$$

$$\frac{\partial^2 v_{11}}{\partial {x_2}^2}-\left(\frac{M^2+\frac{1}{Da}+R_e i\omega}{[1+e_1]}\right)v_{11}=\left(\frac{3e^{2i\omega t}}{[1+e_1]}\right)\left(\frac{\partial v_{10}}{\partial x_2}\right)^2\frac{\partial^2 v_{10}}{\partial {x_2}^2}\qquad\text{(first - order)} \tag{20}$$

The above two equations (19) and (20) are suitable for slip and no-slip condition flow that represent Couette and Poiseuille flow, respectively.

1. For Poiseuille flow (no-slip condition), the two parallel plates are at rest, which means that the boundary conditions in non-dimensional form are $V_1(0)=V_1(1)=0$. After substituting equation $V_1(x_2,t)=v_1(x_2)e^{i\omega t}$ and equation (18) in the boundary conditions and simplifying the result, we have the conditions $v_{10}(0)=v_{10}(1)=0$ for equation (19) and $v_{11}(0)=v_{11}(1)=0$ for equation (20).

2. For Couette flow (slip condition), the lower plate is at rest, while the upper plate is moving with velocity U_h, which means that, the boundary conditions in non-dimensional form are $V_1(0)=0$ and $V_1(1)=U_0$, respectively. After substituting equation $V_1(x_2,t)=v_1(x_2)e^{i\omega t}$ and equation (18) in the boundary conditions and simplifying the result we have the conditions $v_{10}(0)=0, v_{10}(1)=e^{-i\omega t}U_0$ for equation (19) and $v_{11}(0)=v_{11}(1)=0$ for equation (20).

The solution is large in two cases and we will discuss it in the drawings using MATHEMATICA 14.1 software.

B. To solve the heat equation (14) we use the separation of variables method with the boundary condition equation (6). Let $\theta(x_2,t)=\theta_1(x_2)e^{i\omega t}$, where ω represents the oscillation frequency, substituting into equation (14), after simplifying the result, we get:

$$\frac{\partial^2\theta_1}{\partial {x_2}^2}+(N^2-i\omega Pe)\theta_1=-e^{-i\omega t}\left(Br\left([1+e_1]\left(\frac{\partial V_1}{\partial x_2}\right)^2-e_2\left(\frac{\partial V_1}{\partial x_2}\right)^4\right)\right) \tag{21}$$

The solution of equation (21) with boundary conditions $\theta_1(0)=0,\ \theta_1(1)=e^{-it\omega}$ is very large in both cases, and we will discuss it in detail through graphical representations.

C. To solve the concentration equation (15) we use the separation of variables method with the boundary condition equation (7). Let $\Phi(x_2,t)=\ \Phi_1(x_2)e^{i\omega t}$, where ω represents the oscillation frequency, substituting into equation (15), after simplifying the result, we get:

$$\frac{\partial^2\Phi_1}{\partial {x_2}^2}-S_c(K_r+\ i\omega)\Phi_1+S_cS_r\frac{\partial^2\theta_1}{\partial {x_2}^2}=0 \tag{22}$$

The solution of equation (22) with boundary conditions $\Phi_1(0)=0,\ \Phi_1(1)=e^{-it\omega}$ is very large in both cases, and we will discuss it in detail through graphical representations.

Results and Discussion

We discuss the analysis of the MHD oscillatory flow and its effect on the temperature and concentration of Ree-Eyring fluid between two parallel horizontal porous plates, with emphasis on Poiseuille and Couette flows, and present the main results. Numerical evaluations of the analytical results, along with important graphical representations, are shown in Figures (2) to (19). The flow channel area width is defined as $0 \le y \le 1$. The numerical results and figures were generated using Wolfram Mathematica 14.1.

1. The momentum equation was solved using the separation of variables method combined with the perturbation technique, and all results were graphically presented. The movement of the upper wall of the channel at a constant speed ($U_0 = 0.3$) in the case of Couette flow resulted in a higher fluid flow speed within the channel compared to the Poiseuille flow scenario. The velocity patterns for both Poiseuille and Couette flows were illustrated in Figures (2) to (5), which highlighted the influence of various parameters, including the angular frequency (ω), magnetic parameter (M), Reynolds number (Re), parameters (e_1 and e_2), Darcy number (Da), parameter (λ), time (t), and the constant wall speed (U_0), on the fluid velocity. Figure (2) demonstrates that the velocity profile V_1 increases with an increase in the Reynolds number (Re) and parameter (e_2). Similarly, Figure (3) reveals that the velocity profile rises with higher values of the Darcy number (Da) and parameter (λ). In contrast, Figure (4) shows that the velocity decreases as the angular frequency (ω) and parameter (e_1) increase. Finally, Figure (5) indicates that the velocity profile declines with increasing values of the magnetic parameter (M) and time (t).

2. The temperature equation was solved using the method of separation of variables and substitution of the momentum equation into it, and all the results were displayed graphically. The temperature patterns for both Poiseuille and Couette flow were displayed in Figures (6) to (11), which showed the effects of the parameters ω, N, M, Re, e_1, e_2, Da, Pe, β_r, λ, t, i, and U_0 on the fluid temperature profile. Figure (6) shows that the temperature profile increases with the increase in the value of the radiation parameter (N) and the magnetic parameter (M). Figure (7) shows that the temperature increases with the parameter (e_2) and the Brinkman number (β_r). Figure (8) shows the increase in temperature with the increase in the parameter (λ). Conversely, Figure (9) shows that the temperature profile decreases with the increase in the angular frequency (ω) and the Reynolds number (Re). Figure (10) shows a decrease in temperature with the increase in the value of the parameter (e_1) and the Darcy number (Da). Figure (11) indicates a decrease in temperature with increasing Peclet number (Pe) and time (t).

3. The concentration equation was solved using the method of separation of variables and substitution of the momentum equation into it, and all the results were displayed graphically. The concentration patterns for both Poiseuille and Couette flow were displayed in Figures (12) to (19), which showed the effects of the parameters ω, N, M, Re, e_1, e_2, Da, Pe, β_r, Sc, Sr, Kr, λ, t, i, and U_0 on the fluid concentration profile. Figure (12) shows that the concentration profile increases with the angular frequency (ω) and the Reynolds number (Re). Figure (13) shows that the concentration increases with the parameter (e_1) and the Darcy number (Da). Figure (14) shows the increase in concentration with increasing time (t). Conversely, Figure (15) shows that the concentration profile decreases with the increase in the radiation parameter (N) and the magnetic parameter (M). Figure (16) shows a decrease in concentration with the increase in the value of the parameter (e_2) and the Peclet number (Pe). Figure (17) indicates a decrease in concentration with increasing Brinkman number (β_r) and Schmidt number (Sc). Figure (18) indicates a decrease in concentration with increasing Soret number (Sr) and chemical reaction parameter (Kr). Figure (19) indicates a decrease in concentration with the increase in the parameter (λ).

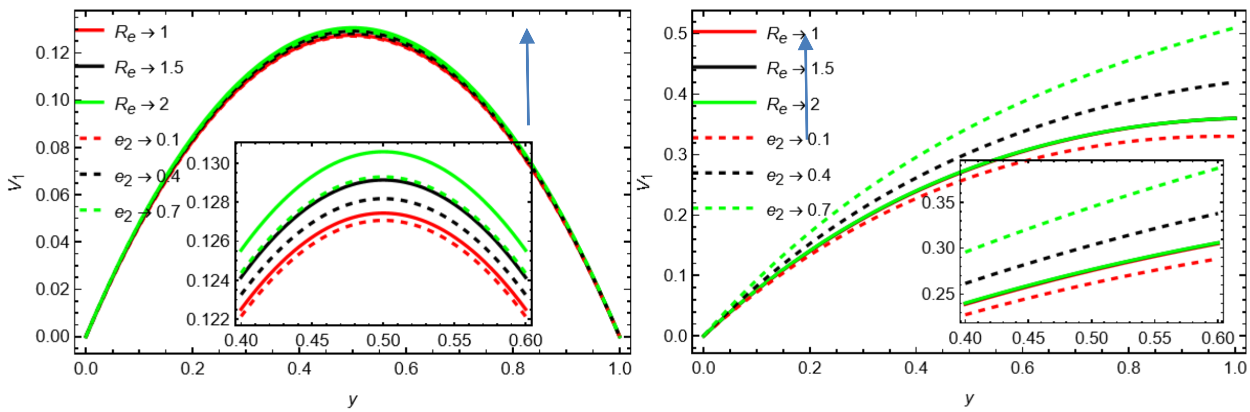

(a) **(b)**

Figure (2) Velocity profile with different values Re = {1, 1.5, 2}, e_2 ={1, 0.4, 0.7} for (a) Poiseuille flow and (b) Couette flow, with ω=1, M =1.2, Da=0.8, $e_1 = 0.5$, t = 0.5, λ = 2, $i = \sqrt{-1}$ and U_0 = 0.3.

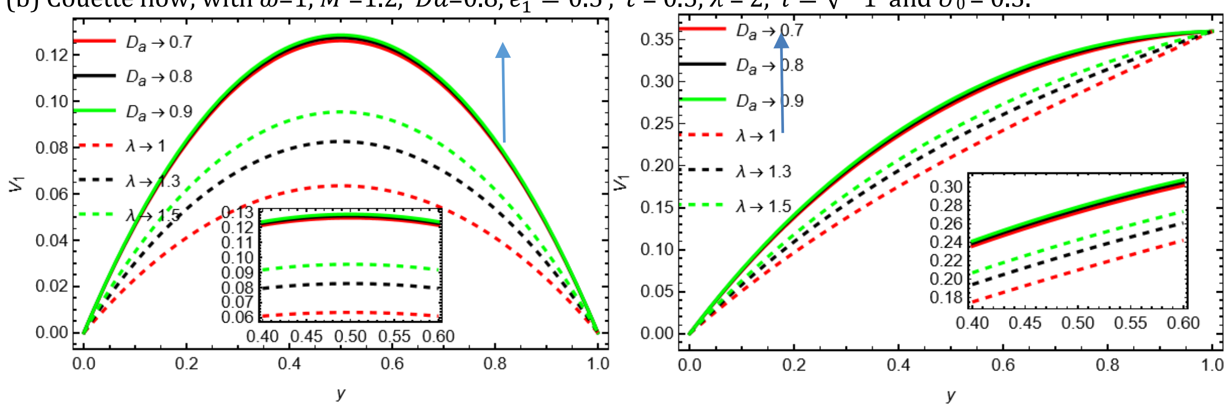

(a) **(b)**

Figure (3) Velocity profile with different values Da = {0.7, 0.8, 0.9}, λ={1, 1.3, 1.5} for (a) Poiseuille flow and (b) Couette flow, with ω=1, Re=1, M =1.2, $e_2 = 0.2$, Da=0.8, t = 0.5, $i = \sqrt{-1}$ and U_0 = 0.3.

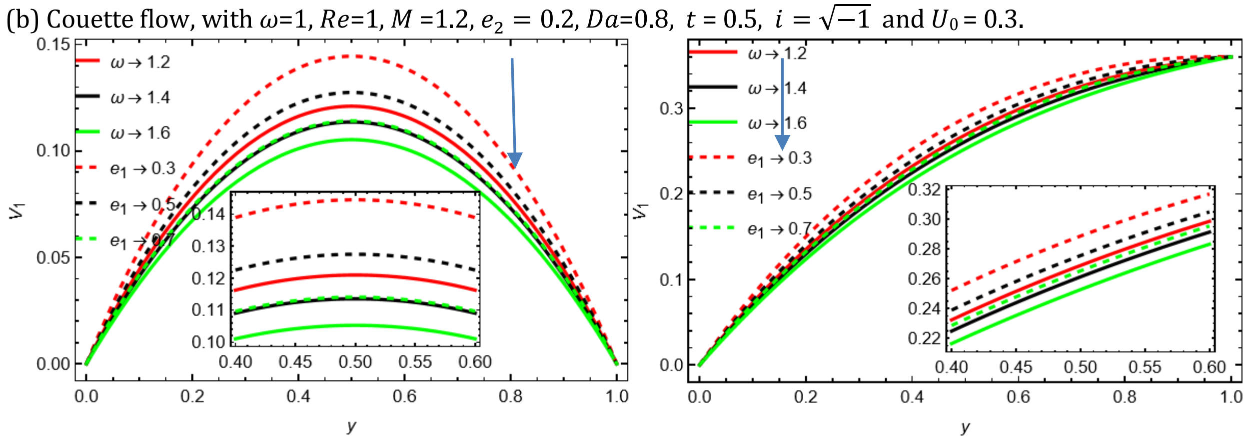

(a) **(b)**

Figure (4) Velocity profile with different values ω = {1.2, 1.4, 1.6}, e_1 = {0.3, 0.5, 0.7} for (a) Poiseuille flow and (b) Couette flow, with Re=1, M =1.2, $e_2 = 0.2$, Da=0.8, λ = 2, t = 0.5, $i = \sqrt{-1}$ and U_0 = 0.3.

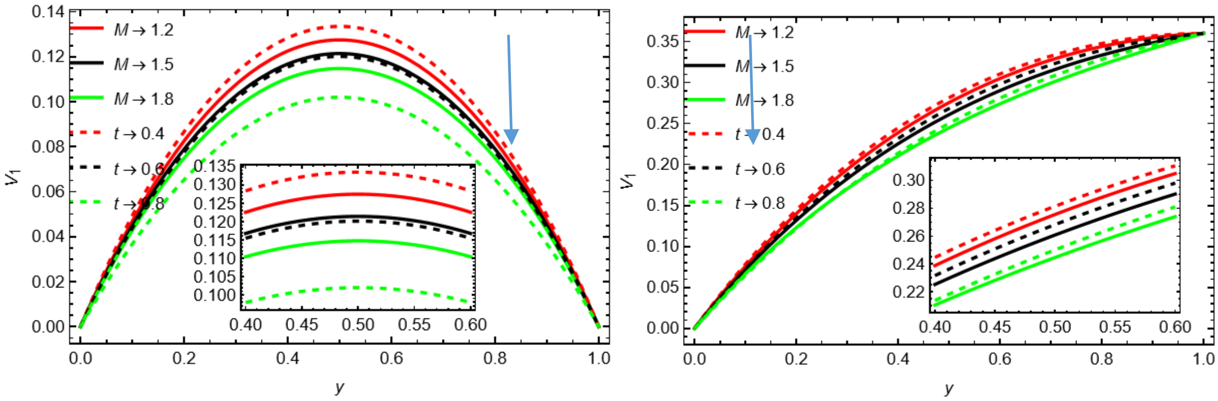

(a) **(b)**

Figure (5) Velocity profile with different values M = {1.2, 1.5, 1.8}, t= {0.4, 0.6, 0.8} for (a) Poiseuille flow and (b) Couette flow, with ω=1, Re=1, $e_1 = 0.5$, $e_2 = 0.2$, Da=0.8, λ = 2, $i = \sqrt{-1}$ and U_0 = 0.3

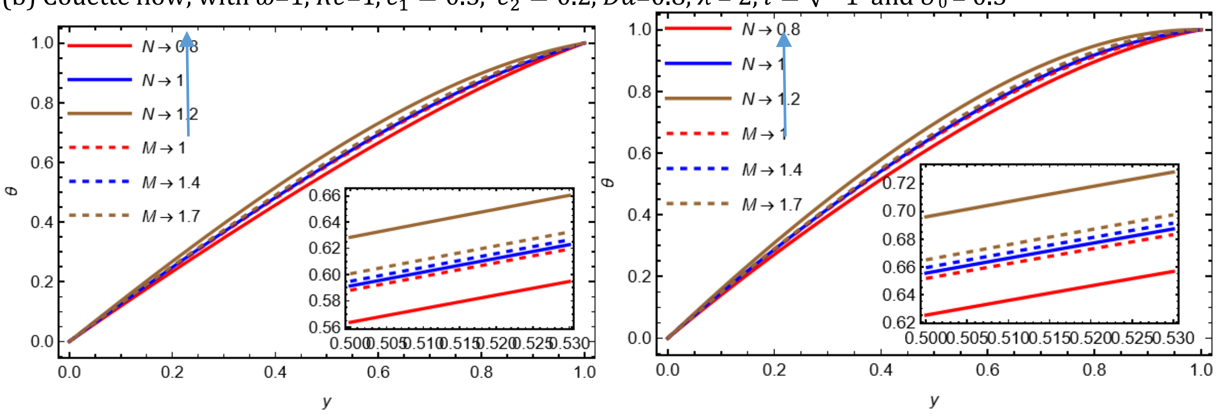

(a) **(b)**

Figure (6) Temperature profile with different values N = {0.8, 1, 0.2}, M= {1, 1.4, 1.7} for (a) Poiseuille flow and (b) Couette flow, with ω=1, Re = 1, $e_1 = 0.5$, $e_2 = 0.2$, $Pe = 0.7$, $\beta_r = 1$, Da=0.8, λ = 2, t = 0.5, $i = \sqrt{-1}$ and U_0 = 0.3.

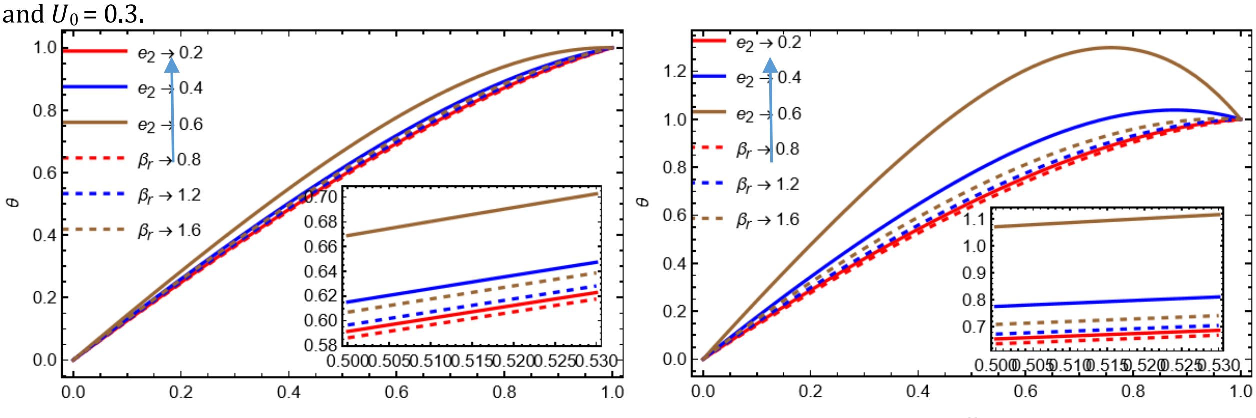

(a) **(b)**

Figure (7) Temperature profile with different values e_2 = {0.2, 0.4, 0.6}, β_r = {0.8, 1.2, 1.6} for (a) Poiseuille flow and (b) Couette flow, with ω=1, N=1, M =1.2, Re = 1, $e_1 = 0.5$, $Pe = 0.7$, Da=0.8, λ = 2, t = 0.5, $i = \sqrt{-1}$ and U_0 = 0.3.

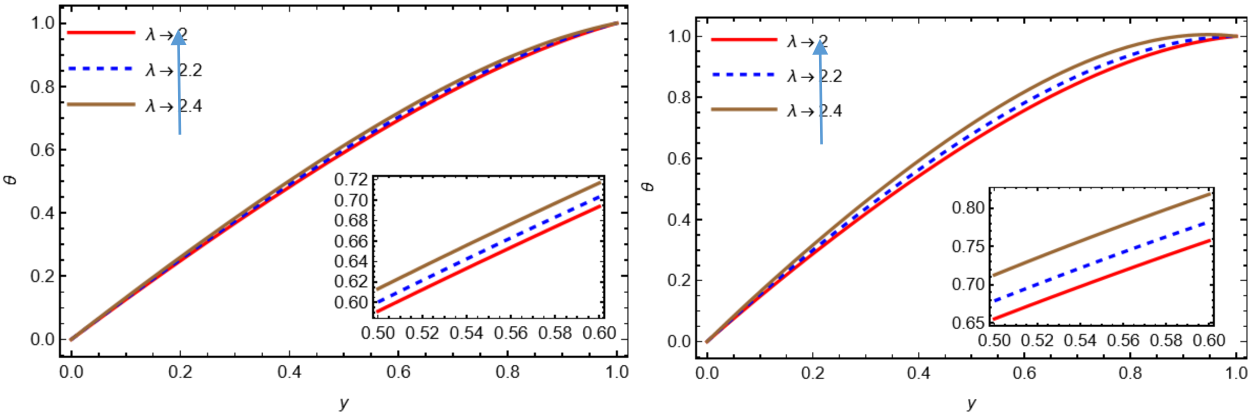

(a) **(b)**

Figure (8) Temperature profile with different values λ = {2, 2.2, 2.4}for (a) Poiseuille flow and (b) Couette flow, with ω=1, *N=1*, M =1.2, Re = 1, $e_1 = 0.5$, $e_2 = 0.2$, $Pe = 0.7$, $\beta_r = 1$, Da=0.8, t = 0.5, $i = \sqrt{-1}$ and U_0 = 0.3.

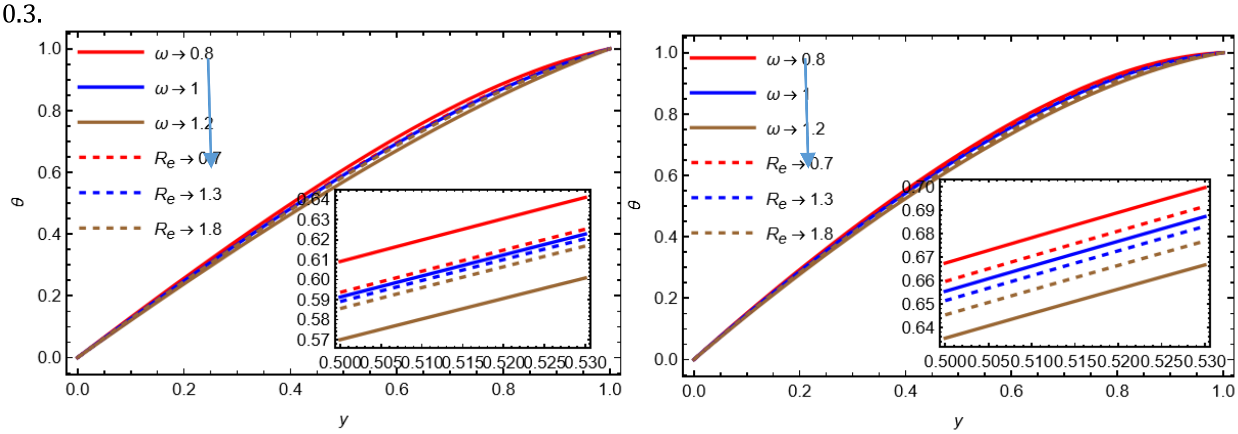

(a) **(b)**

Figure (9) Temperature profile with different values ω ={0.8, 1, 1.2}, ={0.7, 1.3, 1.8} for (a) Poiseuille flow and (b) Couette flow, with *N=1*, M =1.2, $e_1 = 0.5$, $e_2 = 0.2$, $Pe = 0.7$, $\beta_r = 1$, Da=0.8 , λ = 2, t = 0.5, $i = \sqrt{-1}$ and U_0 = 0.3.

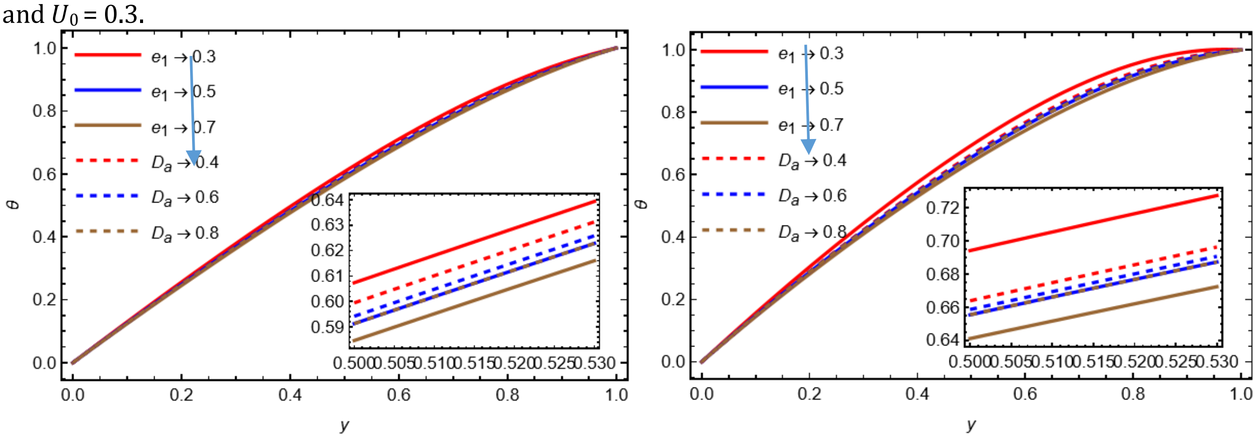

(a) **(b)**

Figure (10) Temperature profile with different values e_1= {0.3, 0.5, 0.7}, Da={0.4, 0.6, 0.8} for (a) Poiseuille flow and (b) Couette flow, with ω=1, *N=1*, M =1.2, Re = 1, $e_2 = 0.2$, $Pe = 0.7$, $\beta_r = 1$, λ = 2, t = 0.5, $i = \sqrt{-1}$ and U_0 = 0.3.

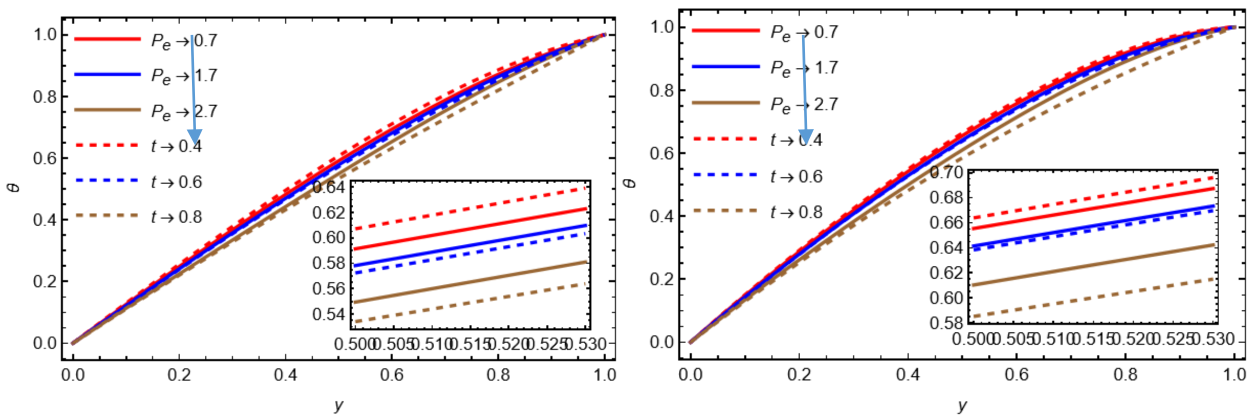

(a) **(b)**

Figure (11) Temperature profile with different values Pe = {0.7, 1.7, 2.7}, t = {0.4, 0.6, 0.8} for (a) Poiseuille flow and (b) Couette flow, with ω=1, N=1, M =1.2, Re = 1, $e_1 = 0.5$, $e_2 = 0.2$, $\beta_r = 1$, Da=0.8, λ = 2, $i = \sqrt{-1}$ and U_0 = 0.3.

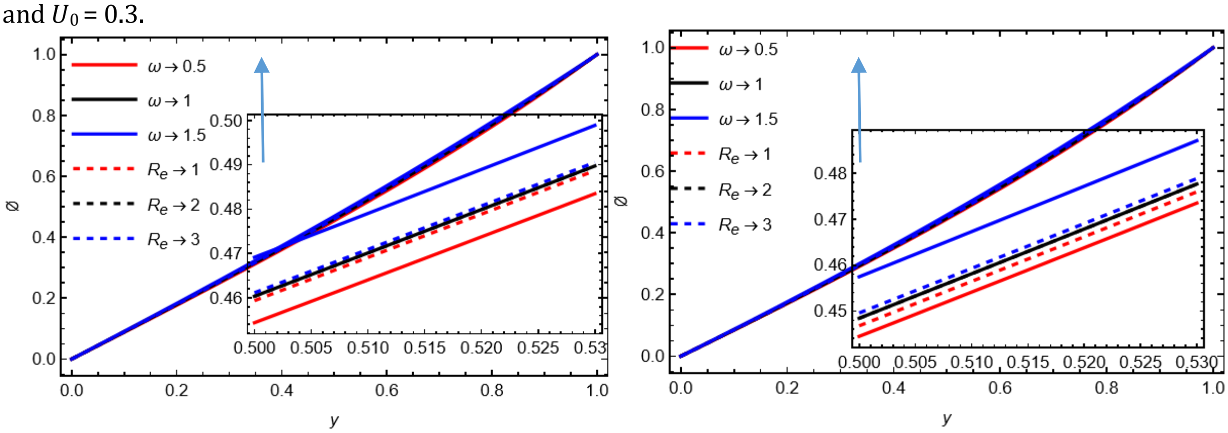

(a) **(b)**

Figure (12) Concentration profile with different values ω = {0.5, 1, 1.5}, Re = {1, 2, 3} for (a) Poiseuille flow and (b) Couette flow, with N=1, M =1.2, $e_1 = 0.5$, $e_2 = 0.2$, $Pe = 0.7$, $\beta_r = 1$, S_c =1, S_r =0.2, K_r =0.3, Da=0.4 , λ = 2, t = 0.5, $i = \sqrt{-1}$ and U_0 = 0.3.

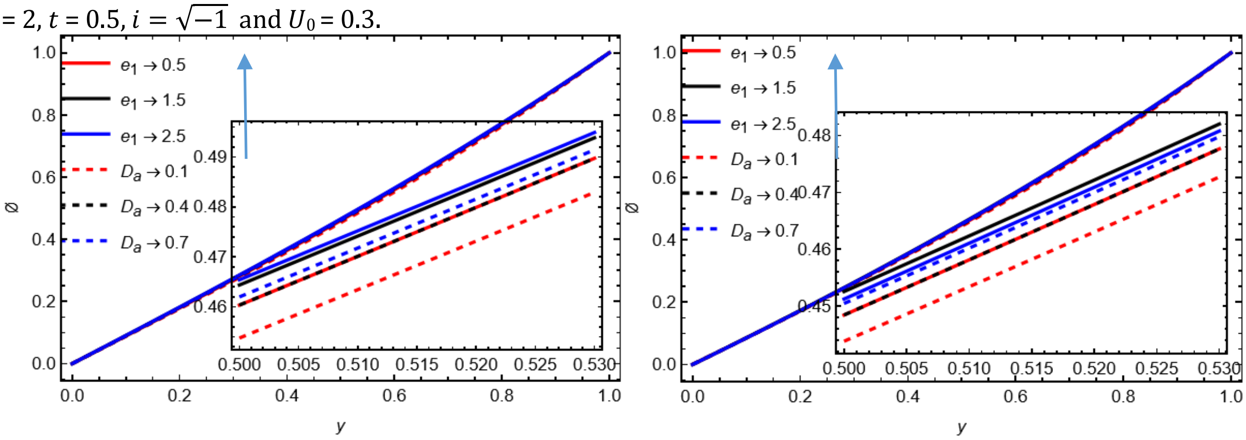

(a) **(b)**

Figure (13) Concentration profile with different values e_1 = {0.5, 1.5, 2.5}, Da = {0.1, 0.4, 0.7} for (a) Poiseuille low and (b) Couette flow, with ω = 1, N=1, M =1.2, Re = 2, $e_2 = 0.2$, $Pe = 0.7$, $\beta_r = 1$, S_c =1, S_r =0.2, K_r =0.3, λ = 2, t = 0.5, $i = \sqrt{-1}$ and U_0 = 0.3.

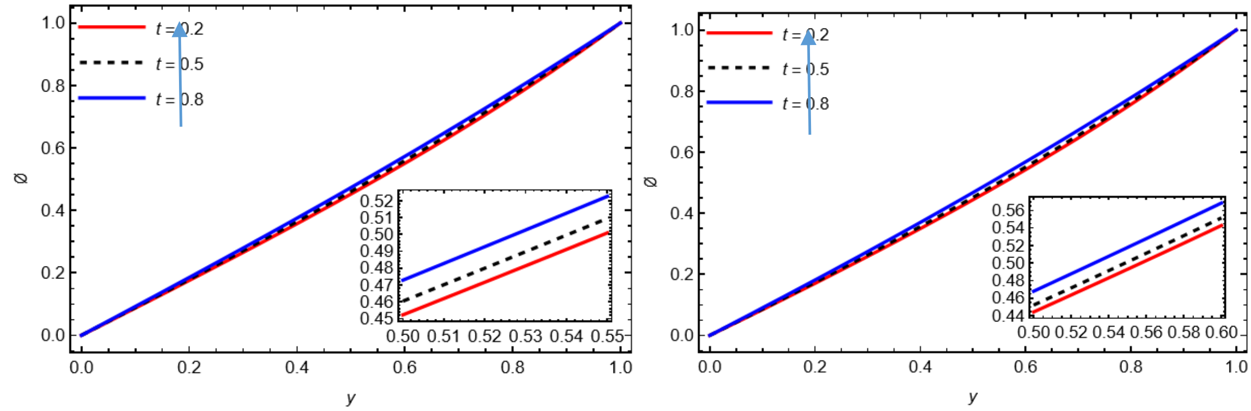

(a) **(b)**

Figure (14) Concentration profile with different values t = {0.2, 0.5, 0.8} for (a) Poiseuille flow and (b) Couette flow, with ω=1, N=1, M =1.2, Re = 2, e_1 = 0.5 , e_2 = 0.2, Pe = 0.7, β_r = 1, S_c =1, S_r =0.2, K_r =0.3, Da=0.4 , λ = 2, $i = \sqrt{-1}$ and U_0 = 0.3.

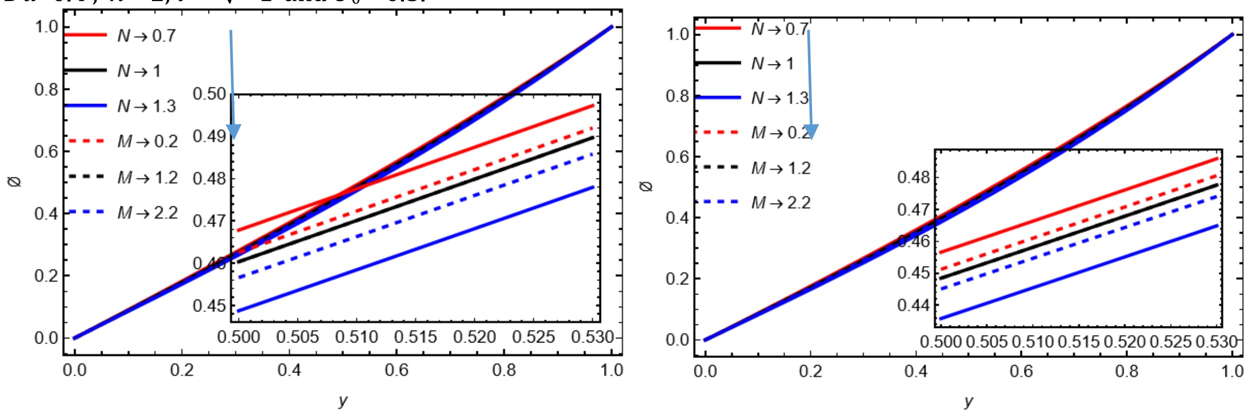

(a) **(b)**

Figure (15) Concentration profile with different values N= {0.7, 1, 1.3}, M = {0.2, 1.2, 2.2} for (a) Poiseuille flow and (b) Couette flow, with ω=1, N=1, M =1.2, Re = 2, e_1 = 0.5 , e_2 = 0.2, Pe = 0.7, β_r = 1, S_c =1, S_r =0.2, K_r =0.3, Da=0.4 , λ = 2, t = 0.5, $i = \sqrt{-1}$ and U_0 = 0.3.

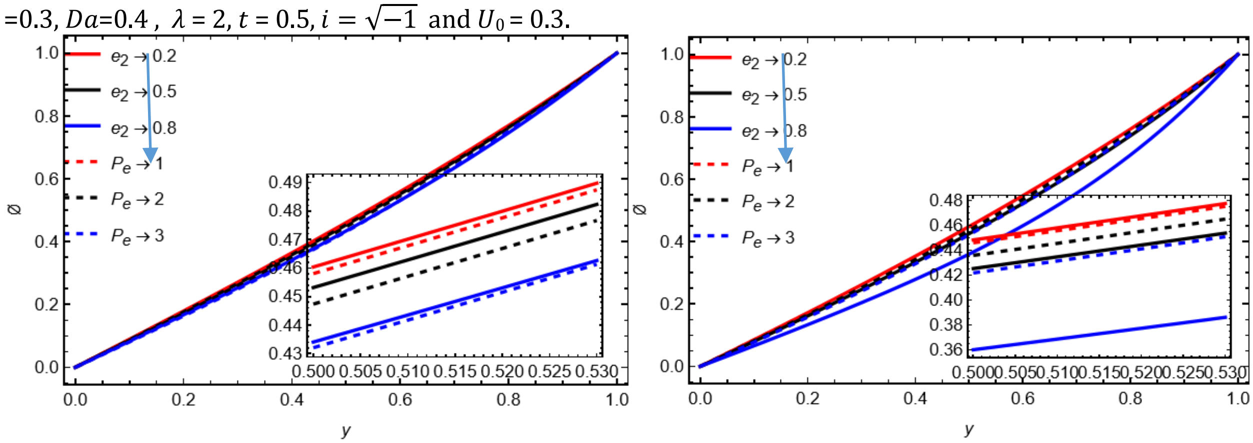

(a) **(b)**

Figure (16) Concentration profile with different values e_2= {0.2, 0.5, 0.8}, Pe = {1, 2, 3} for (a) Poiseuille flow and (b) Couette flow, with ω = 1, N=1, M =1.2, Re = 2, e_1 = 0.5 , β_r = 1, S_c =1, S_r =0.2, K_r =0.3, Da=0.4 , λ = 2, t = 0.5, $i = \sqrt{-1}$ and U_0 = 0.3.

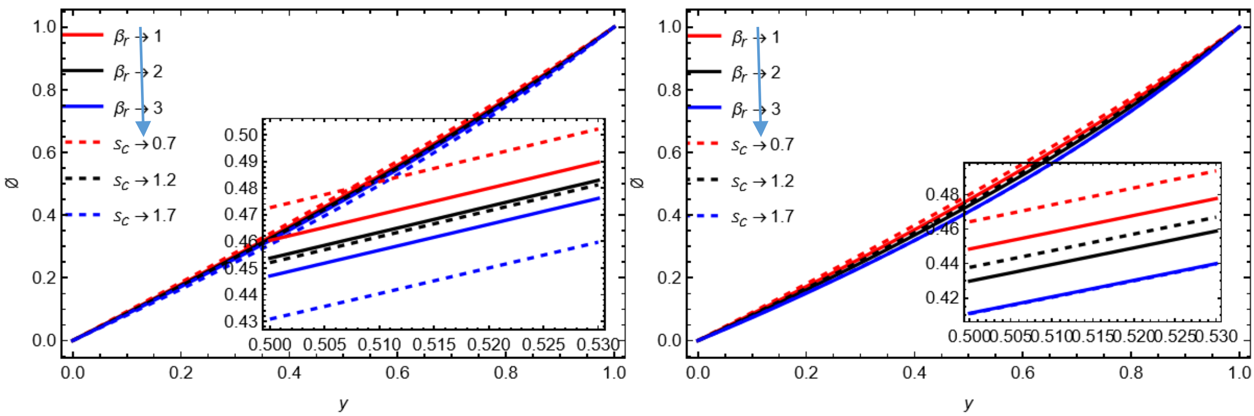

(a) **(b)**

Figure (17) Concentration profile with different values β_r= {1, 2, 3}, S_c ={0.7, 1.2, 1.7} for (a) Poiseuille flow and (b) Couette flow, with ω=1, N=1, M =1.2, Re = 2, $e_1 = 0.5$, $e_2 = 0.2$, $Pe = 0.7$, S_r =0.2, K_r =0.3, Da=0.4 , λ = 2, t = 0.5, $i = \sqrt{-1}$ and U_0 = 0.3.

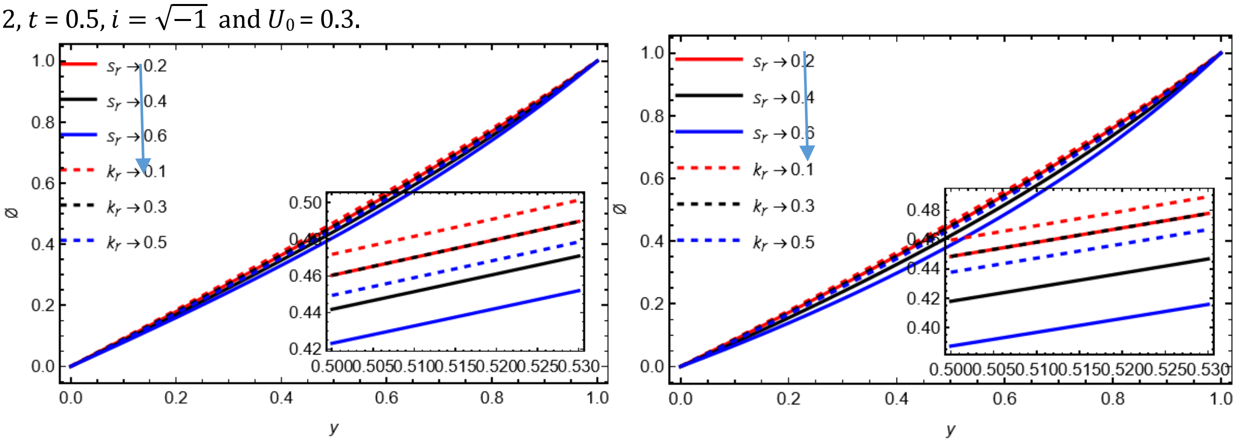

(a) **(b)**

Figure (18) Concentration profile with different values S_r={0.2, 0.4, 0.6}, K_r ={0.1, 0.3, 0.5} for (a) Poiseuille flow and (b) Couette flow, with ω=1, N=1, M =1.2, Re = 2, $e_1 = 0.5$, $e_2 = 0.2$, $Pe = 0.7$, $\beta_r = 1$, S_c =1, Da=0.4 , λ = 2, t = 0.5, $i = \sqrt{-1}$ and U_0 = 0.3.

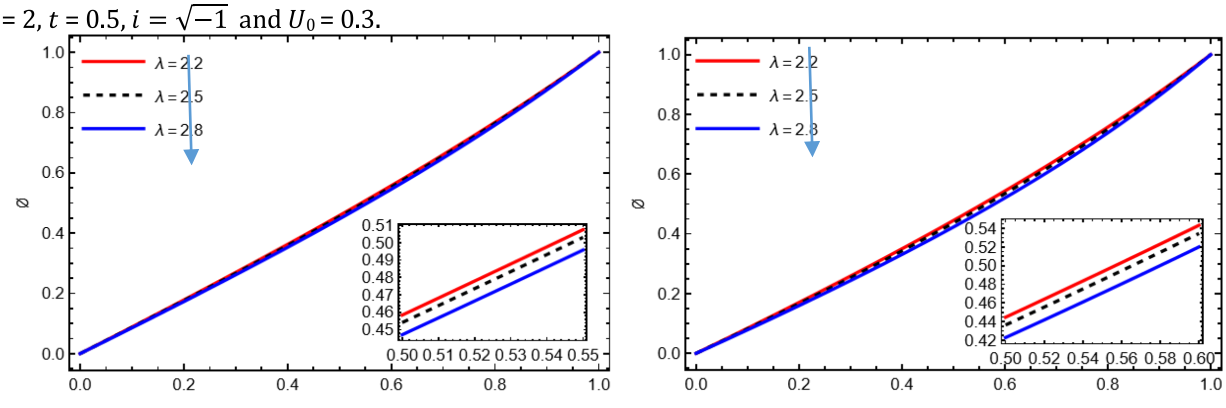

(a) **(b)**

Figure (19) Concentration profile with different values λ={2.2, 2.5, 2.8}for (a) Poiseuille flow and (b) Couette flow, with ω=1, N=1, M =1.2, Re = 2, $e_1 = 0.5$, $e_2 = 0.2$, $Pe = 0.7$, $\beta_r = 1$, S_c=1, S_r=0.2, K_r =0.3, Da=0.4 , t = 0.5, $i = \sqrt{-1}$ and U_0 = 0.3.

Concluding Remarks

In this study, we analyzed the magnetohydrodynamic oscillatory flow and its effect on the temperature and concentration of a Re-Ering fluid between two parallel horizontal porous plates. Using the separation of variables method and turbulence technique, we determined the velocity, temperature and concentration patterns of the fluid. MATHEMATICA 14.1 software was used to discuss the effect of different parameters on fluid motion, temperature and concentration by interpreting the obtained graphs. Different parameter values were used to analyze the results of the relevant parameters, and the main results were highlighted as follows:

- The movement of the upper channel wall at a constant velocity (U_0 = 0.3) in the case of Couette flow increases the fluid flow velocity inside the channel compared to Poiseuille flow.
- The velocity in both Poiseuille and Couette flows increases with the rise in parameters Re, e_2, Da, and λ .
- The velocity in both Poiseuille and Couette flows decreases with the increase in parameters ω, e_1 , M, and t.
- The temperature of the Ree-Eyring fluid increases with increasing N, M, e_2, β_r, and λ but decreases with increasing ω, Re, e_1, Da, Pe, and t in the Poiseuille and Couette flows.

The concentration of the Ree-Eyring fluid increases with increasing ω, Re, e_1, Da, and t but decreases with increasing N, M, e_2 Pe, β_r, S_c, S_r, K_r, and λ in the Poiseuille and Couette flows.

References

[1] Al-Shammari, I. S. S., & Al-Khafajy, D. G. S. Influence of Temperature on the Concentration and thus on the MHD Oscillatory Flow of a Tangent Hyperbolic Fluid through a Regular Permeable Channel. Journal of Al-Qadisiyah for Computer Science and Mathematics 16(2), 36–46 (2024). https://doi.org/10.29304/jqcsm.2024.16.21549

[2] Çengel, Y. A., & Cimbala, J. M. Fluid Mechanics: Fundamentals and Applications (3rd ed.). McGraw-Hill. . (2013). ISBN: 978-0073380322.

[3] Soundalgekar VM and Bhat J. Oscillatory MHD channel flow and heat transfer, Indian Journal of Pure and Applied Mathematics, 15(7), p. 819-828; (1984), ISSN 0019-5588.

[4] Attia, H.A. and Kotb, N.A., MHD flow between two parallel plates with heat transfer, Acta Mechanica, 117, 215–220, (1996). https://doi.org/10.1007/BF01181049

[5] Khudair, W. S. and Dheia, G. Salih Al-khafajy., Influence of heat transfer on Magneto hydrodynamics oscillatory flow for Williamson fluid through a porous medium, Iraqi Journal of Science, 59(1B), 389–397, (2018).

[6] Chhabra, R. P., & Richardson, J. F. Non-Newtonian Flow and Applied Rheology. Engineering Applications Book, Second Edition, (2008). https://doi.org/10.1016/B978-0-7506-8532-0.X0001-7

[7] Bird, R. B., Armstrong, R. C., & Hassager, O. Dynamics of Polymeric Liquids, Volume 1: Fluid Mechanics. Wiley, (1987). https://doi.org/10.1063/5.0196272

[8] Ghosh, S. K. MHD Oscillatory Flow of a Non-Newtonian Fluid in a Porous Medium. International Journal of Heat and Mass Transfer, Volume 108, Pages 1-10, (2017).

[9] Shenoy, A. V. Non-Newtonian Fluid Heat Transfer in Porous Media. Advances in Heat Transfer, Volume 34, Pages 1-50, (1999). https://doi.org/10.1016/S00652717(08)70289-5

[10] Prathiksha Sanil, Rajashekhar Choudhari, Manjunatha Gudekote, Hanumesh Vaidya, Kerehalli Vinayaka Prasad. Impact of Chemical Reactions and Convective Conditions on Peristaltic Mechanism of Ree-Eyring Fluid in a Porous Medium–A Mathematical Model. International Journal of Thermofluids, Volume 26, 101086, March (2025). https://doi.org/10.1016/j.ijft.2025.101086

[11] Ijaz, N., Zeeshan, A., & Bhatti, M. M. Peristaltic propulsion of particulate non-Newtonian Ree-Eyring fluid in a duct through constant magnetic field. Alexandria Engineering Journal, Volume 57, Issue 2, Pages 1055-1060, June (2018). https://doi.org/10.1016/j.aej.2017.02.009

[12] Hayat, T., Akram, J., Alsaedi, A., & Zahir, H. Endoscopy and homogeneous-heterogeneous reactions in MHD radiative peristaltic activity of Ree-Eyring fluid. Results in Physics, Volume 8, Pages 481-488, March (2018). https://doi.org/10.1016/j.rinp.2017.12.056

[13] Haider, I., Jabeen, U., Hussain, A., Mohsin, M. A., Younis, J., Shaaban, I. A., & Assiri, M. A. Viscous dissipation and variable density impact on heat-mass transmission in magneto Ree-Eyring nanofluid across stretched sheet with multiple slips. Case Studies in Thermal Engineering, In Press, Journal Pre-proof, 105871, 13 February (2025). https://doi.org/10.1016/j.csite.2025.105871.